Optimal Wind-Solar Capacity Allocation With Coordination of Dynamic Regulation of Hydropower and Energy Intensive Controllable Load

HONGMING YANG[1,2], (Member, IEEE), QIAN YU[1,2], JUNPENG LIU[1,2],
YOUWEI JIA[3], (Member, IEEE), GUANGYA YANG[4], (Senior Member, IEEE),
EMMANUEL ACKOM[5], AND ZHAO YANG DONG[6], (Fellow, IEEE)

[1]School of Economics and Management, Changsha University of Science and Technology, Changsha 410114, China
[2]International Joint Laboratory of Energy Internet Operation and Planning Based on Distributed Photovoltaic-Storage Energy, Hunan Provincial Engineering Research Center of Electric Transportation and Smart Distribution Network, School of Electrical and Information Engineering, Ministry of Education, Changsha University of Science and Technology, Changsha 410114, China
[3]Department of Electrical and Electronics Engineering, Southern University of Science and Technology, Shenzhen 518055, China
[4]Department of Electrical Engineering, Technical University of Denmark, 2800 Kongens Lyngby, Denmark
[5]UNEP DTU Partnership, Technical University of Denmark, 2100 Copenhagen, Denmark
[6]School of Electrical and Engineering and Telecommunications, University of New South Wales, Sydney, NSW 2052, Australia

Corresponding author: Hongming Yang (yhm5218@163.com)

ABSTRACT With the increasing penetration of renewable energy, it becomes challenging to smoothen highly fluctuant and intermittent power output only through the conventional thermal units. In this paper, by exploiting the dynamic regulating ability of hydropower and energy intensive controllable load to reduce the power output uncertainties, an optimal wind-solar capacity allocation method is proposed. The power regulation characteristics of hydropower stations based on hydraulic head and energy intensive controllable load based on complex production process are modelled. A bi-level (including planning and operation layers) optimization model for wind-solar capacity allocation is proposed, which is subject to the system dynamic regulation constraints. In the planning layer, a cost function model is constructed to minimize the investment and operational cost of the hybrid system with wind-solar, hydropower and energy intensive load. In the operation layer, a coordinated optimal dispatching scheme is proposed to minimize the dynamic source-load tracking coefficient. Finally, case studies on Hunan province China are carried out through four scenarios of various combinations of energy intensive controllable load, system regulation ability and source-load tracking coefficient. The results show the proposed method that taken all of these into account provides better performance in adapting to the power fluctuations, which improves the capacity allocation accuracy of renewable energy and decreases their curtailed amount.

INDEX TERMS Bi-level capacity allocation, hydropower, dynamic regulation, energy intensive controllable load, renewable energy, source-load tracking.

I. INTRODUCTION

As compared to traditional fossil fuel generation, renewable energy (including wind and solar photovoltaic (PV)) owing to its clean and sustainable nature, has become a promising

The associate editor coordinating the review of this manuscript and approving it for publication was Zhouyang Ren.

solution to satisfying the ever-increased load demand. In recent years, wind and solar generation develops rapidly and on a large scale in China. In 2018, the newly installed capacity of wind and solar PV generation has been increased to 20.56 million kW and 44.26 million kW, respectively [1]. However, wind and solar PV generation are highly volatile and intermittent since they are directly affected by the

weather. Thus the high penetration of renewables poses a great challenge to the power system stability [2], [3]. When the regulation capacity of the system is insufficient to dynamically complement the instant power imbalance, the surplus of wind and solar generation should be curtailed to ensure the safe system operational margin [4], [5]. It has been noted that a large amount of wind and solar PV energies are abandoned in China. For instance, the amount of wind power curtailment reaches 27.7 billion kWh, while the one of solar PV reaches 5.49 billion kWh in 2018 [1]. Therefore, it would be admirable to coordinate more available sources and loads to contribute to power balancing in power systems.

Hydropower station (HS) with rapid regulation speed and large storage capacity, is an important schedulable resource in bulk power systems. By controlling the hydraulic head and discharging range, the hydropower generation can regulated timely to assist in smoothing the fluctuated power of wind and solar PV generation [6], [7]. In consideration of this, the regulation ability of HS with a certain reservoir capacity can serve as an important factor in solving the maximization problem of the wind and solar capacity allocation.

In the literature, relevant research works have been investigated on the optimal capacity allocation of hydro-wind-PV hybrid system. An optimal capacity allocation model in the hybrid system is proposed in consideration of the tie-line transmission power constraint [8]. This model is aimed to determine the installed capacity of grid-connected wind and solar PV generation on each bus, of which the objective is to minimize the annual construction cost. However, the constraints of water level or flow limitation of reservoir are considered given merely a single hydropower station. Essential factors (i.e. the inherent characteristics of reservoir storage and the complex hydraulic relationship between upstream and downstream of HS) are unfortunately neglected. In Ref [9], the impacts of reservoir are analyzed on the water level and power output in the downstream. Meanwhile, in considering the storage capacity of the reservoir, the maximum capacity of wind and solar PV generation is determined in the hybrid system. Furthermore, considering the water flow relationship between the upstream and downstream, a coordinated optimization model of renewable energy generation with additional function demands of reservoirs (e.g. irrigation, shipping, flood control, etc.) is constructed in [10], [11]. In the above-mentioned studies, the regulation ability of hydropower generation is rarely reported. Furthermore, the dynamic regulation ability of power variation of HS across time intervals has not been considered to counter-balance the frequent variation induced by wind and solar PV fluctuations.

Similar with the schedulable resources on the generation side, the controllable loads on the demand side have become indispensable resources to participate in system frequency regulation [12], [13]. To this end, the regulation ability of controllable loads is effectively modelled to reflect the two-way interaction between the source and load, and thus increase the installed capacity of wind and solar PV generation.

Admittedly, energy intensive load (EIL) annually consumes large amount of energy, which is equivalent to 5,000 tons of standard coal per year during the productive process [14]. It is with huge regulation capacity (with 0%~80% of the total power capacity) and fast switching ability (i.e. reaching the second level responding rate). Hence, EIL can be effectively dispatched in due course, as compared to other types of controllable loads [15], [16]. By adjusting the production time and planning output, the energy consumption of EIL can be controlled within a certain range. Thereby, the EIL can chip in to facilitate power system frequency stabilization. Inevitably, this would be beneficial to increase the penetration level of renewable generation.

Some recent works have been reported to investigate the involvement of EIL in power system dispatching and renewable energy integration management. The economic benefit and operational cost are analyzed by utilizing EIL regulation. An optimal configuration model with the integration of wind power is presented in [17]. In the response mode, the EIL can be divided into two categories, i.e. i) interruptible loads and ii) translatable loads [18], [19]. A coordinated model considering the regulation ability of controllable loads is constructed to determine the integrated capacity of wind and solar PV generation. The two kinds of EIL i.e. smelting and electrolysis EIL are modelled, and the coordination of wind power and EIL output is discussed in [20]. According to different production period and on/off times, the EILs load characteristics of electrolytic aluminum and poly silicon are modelled in [21], [22]. However, it should be noting that the impacts of productive process on the energy consumption of EIL have been rarely taken into account, as well as the dynamic regulation utilized to respond to the power variation. In addition, in resolving capacity allocation of integrated wind and solar PV power, the coordination between HS and EIL has not been considered to smoothen the power fluctuations induced by wind and solar PV generation.

Therefore, there is an urgent need to develop a capacity allocation approach with source-load interaction, which is capable of smoothing power fluctuations caused by high integration of wind and solar PV generation. In this paper, the dynamic regulation ability of HSs based on hydraulic head and EILs based on complex production process are explicitly modelled in time domain. A bi-level (including planning and operation layers) optimization model for wind and solar PV generation capacity allocation is proposed, of which the objective is to improve the permeation level of renewable power in the hybrid system. The effectiveness and practical feasibility of the proposed method are verified by the extensive case studies based on IEEE 14-bus system, in which the real-world generation and loading profiles in Hunan Province of China are adopted.

II. COORDINATION FRAMEWORK FOR DYNAMIC REGULATION OF SOURCE-LOAD

To timely achieve power balance between load demand and power generation with high penetration of renewables,
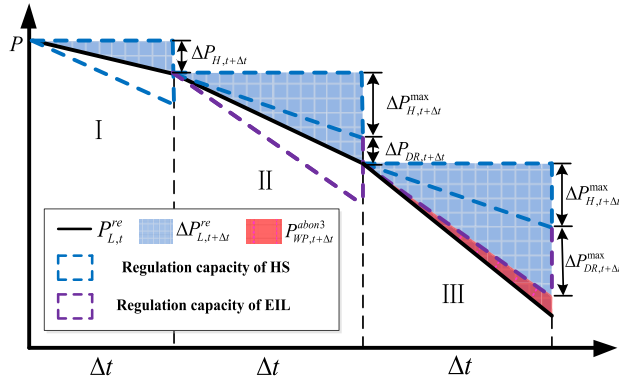
FIGURE 1. Coordinated framework for dynamic regulation of source-load interaction.

a coordination framework of dynamic regulation with source-load interaction (as shown in Fig.1) is proposed, which can assist in smoothing power fluctuations for the whole system. The mechanism behind the framework is twofold. On the one hand, the power output of HS can be efficiently regulated by adjusting the hydraulic head of hydropower units. On the other hand, without affecting the product quality, the power of EIL can be adjusted through tuning the planed output and working state of the smelting furnaces.

The net load of the system is modeled as the subtraction of load demand and negative wind and solar PV generation, which is expressed in Eq (1).

$$P_{L,t}^{re} = P_{L,t} - \left(P_{W,t} + P_{P,t}\right) \tag{1}$$

where $P_{L,t}^{re}$ is the net load power at time t; $P_{L,t}$ is the uncontrollable load power at time t (without EIL); $P_{W,t}$ and $P_{P,t}$ denote the wind and solar PV power at time t, respectively. When $P_{L,t}$ is invariable, the penetration level of wind and solar PV generation power of the system can be increased along with the decrease of $P_{L,t}^{re}$.

At the system operation stage, the power balance between supply and demand at time t is expressed as,

$$P_{L,t}^{re} = P_{G,t} + P_{H,t} - P_{DR,t} \tag{2}$$

where $P_{G,t}$ is the generation power of thermal units at time t; $P_{H,t}$ is the generation power of HS at time t; $P_{DR,t}$ denotes the controllable load power of EIL at time t.

The power fluctuation of the net load from the wind and solar PV generation power output from time t to $t+\Delta t$ occurs, i.e.

$$\Delta P_{L,t+\Delta t}^{re} = P_{L,t}^{re} - P_{L,t+\Delta t}^{re} \tag{3}$$

where Δt is the dispatch time interval. $\Delta P_{L,t+\Delta t}^{re}$ should be balanced by the dispatchable resource. Otherwise, $\Delta P_{L,t+\Delta t}^{re}$ would become the curtailed amount of wind and solar PV generation, denoted by $\Delta P_{L,t+\Delta t}^{re} = P_{WP,t+\Delta t}^{abon1}$.

In order to reflect the regulation effects of HS and EIL towards the fluctuations, the generation power of thermal units is assumed to be unchanged and represented

as $P_{G,t} = P_{G,t+\Delta t}$. In case that the regulation power of HS is considered, one can obtain,

$$\Delta P_{L,t+\Delta t}^{re} + \Delta P_{H,t+\Delta t} = P_{G,t} + P_{H,t} - P_{DR,t} - P_{L,t+\Delta t}^{re} + \Delta P_{H,t+\Delta t} \tag{4}$$

where $\Delta P_{H,t+\Delta t}$ represents the regulation power of HS from time t to $t + \Delta t$. If the HS is with large regulation capacity, $P_{WP,t+\Delta t}^{abon1}$ can be fully compensated by the HS (shown in area I in Fig. 1), i.e.

$$P_{WP,t+\Delta t}^{abon1} = \left| \Delta P_{H,t+\Delta t} \right| \tag{5}$$

If the power fluctuation of net load is greater than the regulation power of HS while $\Delta P_{H,t+\Delta t}$ is reduced to its minimum technical output $\Delta P_{H,t+\Delta t}^{max}$ (as shown in the area II in Fig. 1), i.e. $P_{H,t+\Delta t} = P_{H,\min}$, the curtailed amount $P_{WP,t+\Delta t}^{abon2}$ of wind and solar PV generation by regulating the hydro generation units is expressed as,

$$P_{WP,t+\Delta t}^{abon2} = \Delta P_{L,t+\Delta t}^{re} + \Delta P_{H,t+\Delta t} \tag{6}$$

If the regulation power of EIL is further utilized, it becomes,

$$\Delta P_{L,t+\Delta t}^{re} + \Delta P_{H,t+\Delta t} - \Delta P_{DR,t+\Delta t} = P_{G,t} + P_{H,t} - P_{DR,t} - P_{L,t+\Delta t}^{re} + \Delta P_{H,t+\Delta t} - \Delta P_{DR,t+\Delta t} \tag{7}$$

where $\Delta P_{DR,t+\Delta t}$ represents the up regulation power of EIL from time t to $t+\Delta t$. If the EIL has large regulation capacity, $P_{WP,t+\Delta t}^{abon2}$ can be fully compensated by the EIL, i.e.

$$P_{WP,t+\Delta t}^{abon2} = \Delta P_{DR,t+\Delta t} \tag{8}$$

If the EIL is increased to its maximum regulation capacity (as shown in area III in Fig. 1), i.e. $P_{DR,t+\Delta t} = P_{DR,\max}$, the curtailed amount $P_{WP,t+\Delta t}^{abon3}$ of wind and solar PV generation by regulating the power of hydro generation units and controllable loads is expressed as,

$$P_{WP,t+\Delta t}^{abon3} = \Delta P_{L,t+\Delta t}^{re} + \Delta P_{H,t+\Delta t} - \Delta P_{DR,t+\Delta t} \tag{9}$$

Lastly, $P_{WP,t+\Delta t}^{abon3}$ is covered by the thermal unit within its regulation range to maintain the power balance for the whole system. By taking advantage of regulation capacity of HS and EIL, the system can smoothen the generation power of thermal units to the greatest extent, through which frequent on/off actions can be avoided. The larger dynamic regulation capacity of HS and EIL is, the more the wind and solar PV generation can be integrated into the system.

Therefore, the dynamic regulation ability of the system is crucial for the penetration level of wind and solar PV generation. It is thus of vital importance to accurately model the dynamic source-load regulation capability to facilitate capacity allocation of wind and solar PV generation.

III. DYNAMIC REGULATION MODELLING OF SOURCE-LOAD INTERACTION

A. DYNAMIC REGULATION MODELLING OF HS

The HS with reservoir can adjust the downstream discharge by changing the hydraulic head, with satisfying the complex hydraulic constraints of upstream and downstream. If the downstream discharge is smaller than the upstream inflow (i.e. the difference between discharge and interval inflow of the upstream hydropower station), the water level in the reservoir rises. Thus, the water storage is increased to reduce the power output of HS under satisfaction of the system dispatch requirement, and vice versa.

The power output of HS is modeled as,

$$P_{H,n,t} = g\eta_n Q_{n,t} H_{n,t} \tag{10}$$

where $P_{H,n,t}$ is the power output of HS at bus n at time t; $Q_{n,t}$, $H_{n,t}$ are the generating discharge and hydraulic head of HS at bus n at time t, respectively; η_n indicates the corresponding generating efficiency.

The power output of HS mainly depends on the hydraulic head and the generating discharge, as expressed in (10). According to the dynamic equations of the hydraulic turbine units, the relationship between the hydraulic head and the generating discharge can be expressed as follows,

$$Q_{n,t} = kG_n\sqrt{H_{n,t}} \tag{11}$$

$$H_{n,t} = H_{n,0} - H_{n,t}^{loss} \tag{12}$$

$$H_{n,t}^{loss} = f_n G_n^2 H_{n,t} \tag{13}$$

where, G_n is the guide vane opening of HS; k represents the proportion coefficient; $H_{n,0}$ is the initial hydraulic head; $H_{n,t}^{loss}$ is the hydraulic head loss at time t; f_n indicates the loss coefficient due to pipe friction.

Thus, the intrinsic relationship can be expressed as:

$$Q_{n,t} = kG_n\sqrt{\left(H_{n,0} - f_n G_n^2 H_{n,t}\right)} \tag{14}$$

One can substitute Eq. (14) into Eq. (10). The power output of HS varies with hydraulic head, which is represented by

$$P_{H,n,t} = \left(kg\eta_n G_n H_{n,0}/\left(1 + f_n G_n^2\right)\right) H_{n,t}^{0.5} \tag{15}$$

By using Taylor expansion at $H_{n,t-1}$, one can obtain,

$$P_{H,n,t} = P_{H,n,t-1} + 0.5K_H H_{n,t-1}^{-0.5} \left(H_{n,t} - H_{n,t-1}\right) \\ - 0.125K_H H_{n,t-1}^{-1.5} \left(H_{n,t} - H_{n,t-1}\right)^2 + \cdots \tag{16}$$

where $K_H = \left(kg\eta_n G_n H_{n,0}\right)/\left(1 + f_n G_n^2\right)$. By neglecting the quadratic and higher-order terms, Eq (13) can be simplified as

$$P_{H,n,t} - P_{H,n,t-1} = 0.5K_H H_{n,t-1}^{-0.5} \left(H_{n,t} - H_{n,t-1}\right) \tag{17}$$

That is, the relationship between the power variation $\Delta P_{H,n,t}$ and the hydraulic head $\Delta H_{n,t}$ is

$$\Delta P_{H,n,t} = 0.5K_H H_{n,t-1}^{-0.5} \Delta H_{n,t} \tag{18}$$

With the practical constraints of maximum/minimum technical output and ramp-up/ramp-down rate, the maximum up/down regulation power of HS is varied with hydraulic head, which can be expressed as,

$$\begin{cases} \Delta P_{H,n,t+\Delta t}^+ \\ = \min(P_{H,n,\max} - P_{H,n,t}, 0.5K_H H_{n,t}^{-0.5}\Delta H_{n,t+\Delta t}^{up}) \\ \Delta P_{H,n,t+\Delta t}^- \\ = -\min(P_{H,n,t} - P_{H,n,\min}, 0.5K_H H_{n,t}^{-0.5}\Delta H_{n,t+\Delta t}^{dw}) \end{cases} \tag{19}$$

where $\Delta P_{H,t+\Delta t}^+$, $\Delta P_{H,t+\Delta t}^-$ are the up/down regulation power of HS at bus n from time t to $t + \Delta t$, respectively; $P_{H,n,\max}$, $P_{H,n,\min}$ are the upper/lower bounds of power output, respectively; $\Delta H_{n,t+\Delta t}^{up}$, $\Delta H_{n,t+\Delta t}^{dw}$ are the maximum adjustment of up/down hydraulic head at time $t + \Delta t$.

B. DYNAMIC REGULATION MODELLING OF EIL

EIL with fast responding rate and large regulation capacity typically serves as an important schedulable resource on the demand side. There are many types of EIL with different energy consumption characteristics. For example, the smelting load (ferroalloy, aluminum smelting and silicon carbide) with discretized regulation. The up/down regulation power can be obtained by adjusting the tradeoff between the production process and the energy consumption.

The smelting furnace is the main energy consumption equipment in the entire smelting EIL. The production process including three states of smelting furnace is shown in Fig. 2.
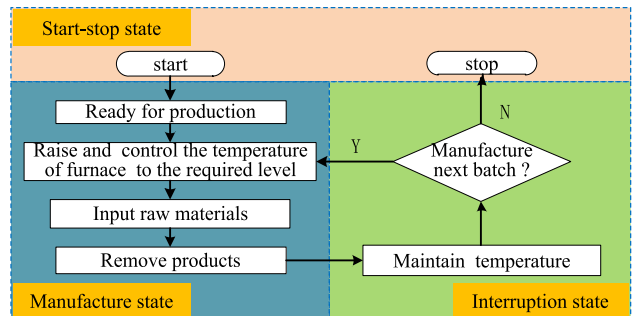
FIGURE 2. The production process including three states of smelting furnace.

Due to the high startup and shutdown cost for the smelting EIL, the power can be regulated during the manufacture and interruption states, i.e.

$$P_{DR,n,t} = P_{DR,n,t}^{off}(1 - x_{DR,n,t}) + P_{DR,n,t}^{on}x_{DR,n,t} + \Delta P_{DR,n,t} \tag{20}$$

where $P_{DR,n,t}$ is the load power of smelting furnaces at bus n at time t; $x_{DR,n,t}$ is a 0–1 state variable, 1 represents the state that the batch is manufacturing, and 0 represents the interruption state; $P_{DR,n,t}^{off}$, $P_{DR,n,t}^{on}$ are the corresponding load power at the two states; $\Delta P_{DR,n,t}$ is the regulation power of smelting furnaces at time t, which is obtained by the planned output of each furnace.

The regulation power should be within the acceptable range of the designed capacity of smelting furnace, i.e.

$$-\Delta P_{DR,n,\max}^{dw}x_{DR,n,t} \le \Delta P_{DR,n,t+\Delta t} \le \Delta P_{DR,n,\max}^{up}x_{DR,n,t} \tag{21}$$

where $\Delta P^{up}_{DR,n,t+\Delta t,\max}$, $\Delta P^{dw}_{DR,n,t+\Delta t,\max}$ are the maximum up/down regulation power of EIL, respectively. The up/down regulation power of smelting furnace at manufacture state from time t to $t+\Delta t$ is related to the EIL load power at time t.

$$\Delta P^{dw}_{DR,n,t+\Delta t,\max} = P^{on}_{DR,n,t} - P^{on}_{DR,n,\min} \qquad (22)$$

$$\Delta P^{up}_{DR,n,t+\Delta t,\max} = P^{on}_{DR,n,\max} - P^{on}_{DR,n,t} \qquad (23)$$

Therefore, the load power of smelting furnaces should be within the acceptable range

$$P^{on}_{DR,n,\min} \leq P_{DR,n,t} \leq P^{on}_{DR,n,\max} \qquad (24)$$

where $P^{on}_{DR,n,\max}$, $P^{on}_{DR,n,\min}$ are the upper/lower power bounds.

In addition, the down regulation power at interruption state would make the furnace temperature lower than the required value to reduce the product quality. Thus, the EIL at interruption state only participates to the up power regulation.

Considering the planned output and the two working states of interruption and manufacture, the up/down regulation ability of smelting EIL can be modeled as Eq (22).

$$
\begin{cases}
\Delta P^{+}_{DR,t+\Delta t} \\
= \min
\begin{pmatrix}
\Delta P^{up}_{DR,n,t+\Delta t,\max}x_{DR,n,t} \\
+(P^{on}_{DR,n,\max} - P^{off}_{DR,n,t})(1 - x_{DR,n,t}), \\
r^{up}_{DR,n,t}\Delta t + P^{off}_{DR,n,t}(1 - x_{DR,n,t})
\end{pmatrix} \\
\Delta P^{-}_{DR,t+\Delta t} \\
= -x_{DR,n,t}\left(\min(\Delta P^{dw}_{DR,n,t+\Delta t,\max}, r^{dw}_{DR,n,t}\Delta t)\right)
\end{cases}
\qquad (25)
$$

where $\Delta P^{+}_{DR,t+\Delta t}$, $\Delta P^{-}_{DR,t+\Delta t}$ are the up/down regulation power from time t to $t + \Delta t$, respectively; $r^{up}_{DR,n,t}$, $r^{dw}_{DR,n,t}$ are the maximum up/down ramp rate limitation at time t.

C. DYNAMIC REGULATION MODELLING OF HS AND EIL COORDINATION

When the regulation capacity of the system is lower than the fluctuated power of wind and solar PV generation, the curtailment of renewable energy would be in place. Therefore, based on the source-load coordination between the HS and EIL, the up/down regulation ability of the system should satisfy the up/down power regulation constraints of the net load, which can be expressed as

$$
\begin{cases}
\Delta P^{+}_{H,t+\Delta t} + \left|\Delta P^{-}_{DR,t+\Delta t}\right| \geq \Delta P^{re}_{L,t+\Delta t} & \Delta P^{re}_{L,t+\Delta t} \geq 0 \\
\left|\Delta P^{-}_{H,t+\Delta t}\right| + \Delta P^{+}_{DR,t+\Delta t} \geq \left|\Delta P^{re}_{L,t+\Delta t}\right| & \Delta P^{re}_{L,t+\Delta t} < 0
\end{cases}
\qquad (26)
$$

IV. BI-LEVEL OPTIMIZATION OF WIND-SOLAR CAPACITY ALLOCATION BASED ON SOURCE-LOAD DYNAMIC REGULATION

A bi-level optimization model of wind-solar capacity allocation is constructed based on the dynamic regulation ability of HS and EIL. The objective is to maximize the penetration level of renewables and minimize the overall cost of the system, as illustrated in Fig. 3. The upper planning layer
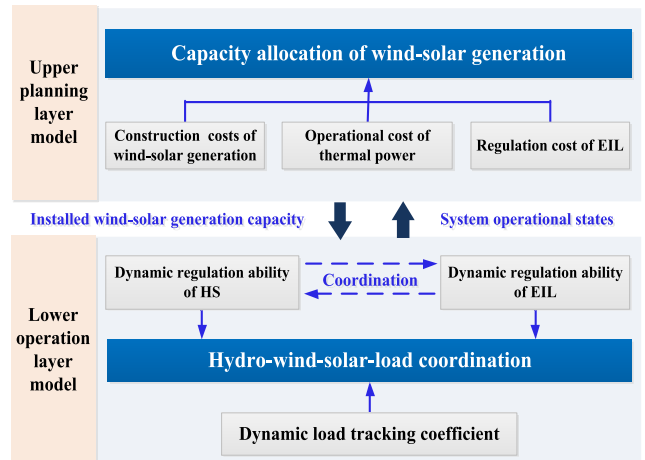

FIGURE 3. Bi-level optimization framework of capacity allocation.

is aimed to maximize the installed capacity of wind and solar PV generation within the system dynamic regulation ability. The lower operation layer is aimed to minimize the dynamic load tracking coefficient to achieve the coordinated scheduling of the hybrid system. The upper and lower layers are closely coupled by the decision variables covering the installed wind-solar generation capacity and system operational states.

A. THE UPPER PLANNING LAYER MODEL
The objective of the upper-layer model is to minimize the overall cost of the hybrid system, which covers the investment cost of wind and solar PV generation and operational cost of EIL and conventional thermal power. The operational cost of HS, wind and solar PV generation are ignored in this model due to their value are relatively small and nearly constant in the operation condition. The objective function is modeled as:

$$\min F_1 = C_{CON} + C_{DR} + C_G \qquad (27)$$

The annualized construction cost of wind and solar PV generation is amortized over the total investment costs during the entire life span to each year at the rate of depreciation, which can be formulated as:

$$C_{CON} = \sum_{n=1}^{N}\left[\frac{d(1+d)^{T_{LS}}}{(1+d)^{T_{LS}} - 1}\right](c_W S_{W,n} + c_P S_{P,n}) \qquad (28)$$

where $S_{W,n}$, $S_{P,n}$ are the installed capacity of wind and solar PV generation at bus n, respectively; c_W, c_P are the corresponding investment price per unit of installed capacity; d denotes the rate of depreciation; T_{LS} represents the entire life span, for example here it is set as 15 years; N is the number buses of the system.

The regulation cost of EIL is

$$C_{DR} = \sum_{n=1}^{N}\sum_{t=1}^{8760} c_{DR}P_{DR,n,t} \qquad (29)$$

where c_{DR} represents the unit power regulation cost of EIL.

The operational cost of conventional thermal power is

$$C_G = \sum_{n=1}^{N} \sum_{t=1}^{8760} \left(a_n P_{G,n,t}^2 + b_n P_{G,n,t} + c_n \right) \quad (30)$$

where a_n, b_n, c_n are the cost coefficient of thermal generation; $P_{G,n,t}$ is the generation power of thermal unit at bus n at time t.

The decision variables of the upper-layer optimization include the installed capacity of wind-PV generation, which are subject to the maximum installed capacity constraints.

B. THE LOWER OPERATION LAYER MODEL

The load tracking coefficient is introduced to represent the matching degree of the variation between the fluctuant power and controllable power. In the operation layer, the dynamic load tracking coefficient is proposed to reflect the amplitude of integrated wind-PV generation, as (1), but also the dynamic regulation ability of HS and EIL in smoothing the fluctuations induced by wind and solar PV during a certain period of time, as expressed in Eq (9).

The objective of the lower operation layer is to minimize the dynamic load tracking coefficient, in which min-max normalization is employed [23]. The normalization of dynamic load tracking coefficient is expressed as

$$\min F_2 = \sum_{t=1}^{8760} \sum_{n=1}^{N} \frac{\left(\left| P_{WP,n,t+\Delta t}^{abon3} \right| - \left| P_{WP,n,t+\Delta t}^{abon3,\min} \right| \right)}{\left(\left| P_{WP,n,t+\Delta t}^{abon3,\max} \right| - \left| P_{WP,n,t+\Delta t}^{abon3,\min} \right| \right)}$$
$$+ \frac{\left(\left| P_{L,n,t}^{re} \right| - \left| P_{L,n,t}^{re,\min} \right| \right)}{\left(\left| P_{L,n,t}^{re,\max} \right| - \left| P_{L,n,t}^{re,\min} \right| \right)} / 8760 \quad (31)$$

If the dynamic load tracking coefficient F_2 becomes smaller, HS and EIL can provide better performance in tracking the power variation of wind and solar PV generation. In this sense, system integrates larger permeation of renewable energy even if the generation power of thermal units changes slightly.

The lower-layer model ensures the optimal operation of the system under a certain capacity allocation level to coordinate the operational states of wind, solar PV, HS and EIL. The decision variables of the lower-layer optimization model are the power output of HS, EIL and thermal units. The formulated optimization is subject to specific constraints for both dynamic and static states. The dynamic constraints include

i) The proposed system dynamic regulation ability as expressed in Eq (26);

ii) The upper and lower bounds of EIL regulation power at manufacture state, as expressed in Eq (21);

iii) The upstream and downstream flow balance of HS

$$\begin{cases} Q_{n,t}^{in} = I_{n,t} + Q_{n+1,t-\tau_n} \\ V_{n,t} = V_{n,t-1} + 3600 \times \left(Q_{n,t}^{in} - Q_{n,t} - S_{n,t} \right) \Delta t \end{cases} \quad (32)$$

where $Q_{n,t}^{in}$ is the inflow of HS at time t at bus n; $I_{n,t}$ is the interval inflow of HS at time t at bus n; $Q_{n+1,t-\tau_n}$ is the

discharged flow of HS at time $t - \tau_n$ at bus $n + 1$; τ_n is time delay of HS flow at bus $n + 1$ to bus n. Its value is positively correlated with the actual distance between the upper and lower HS. $V_{n,t}$ and $V_{n,t-1}$ are the spillage of downstream HS at time t and time $t - 1$ at bus n; $S_{n,t}$ is the discarded water of HS at time t at bus n.

In addition, the static constraints include

i) The system power balance

$$\sum_{n=1}^{N} P_{W,n,t} + \sum_{n=1}^{N} P_{P,n,t} + \sum_{n=1}^{N} P_{G,n,t}$$
$$= \sum_{n=1}^{N} P_{L,n,t} + \sum_{n=1}^{N} P_{DR,n,t} \quad (33)$$

ii) The transmission line thermal limits

$$P_l < P_l^{\max} \quad (34)$$

where P_l is the power flow transmission of line l; $P_l^{\max}$ is the upper limit on power flow transmission of line l.

iii) The upper and lower bounds of wind and solar PV generation

$$\begin{cases} 0 \le P_{W,n,t} \le \zeta S_{W,n} \\ 0 \le P_{P,n,t} \le \zeta S_{P,n} \end{cases} \quad (35)$$

where ζ is the coefficient of maximum technical output of wind and solar PV generation, which is valued 0.9 generally.

iv) The upper and lower bounds of reservoir capacity and hydraulic head

$$\begin{cases} V_{n,0} = V_n^{Begin} \\ V_{n,T} = V_n^{End} \end{cases} \quad (36)$$

$$\begin{cases} V_n^{\min} \le V_{n,s,t} \le V_n^{\max} \\ H_{n,\min} \le H_{n,t} \le H_{n,\max} \end{cases} \quad (37)$$

where $V_{n,0}$ and $V_{n,T}$ are the reservoir capacity at time 0 and time t at bus n; V_n^{Begin} and V_n^{End} are the initial and end reservoir capacity at bus n; $V_n^{\min}$ and $V_n^{\max}$ are the minimum and maximum spillage capacity of HS at bus n; $H_{n,\min}$, $H_{n,\max}$ are the minimum and maximum hydraulic head of HS at bus n, respectively.

v) The required production quantity of EIL

$$\sum_{n=1}^{N} \sum_{t=1}^{T} \tau_n P_{DR,n,t} \Delta t \ge o_{EIL} \quad (38)$$

where τ_n is the coefficient of unit production quantity of EIL at bus n, which can be obtained by the linearization curve of load power and production quantity of smelting furnaces; o_{EIL} is the required production quantity of EIL.

vi) The maximum technical output of the thermal units.

$$P_{G,n}^{\min} \le P_{G,n,t} \le P_{G,n}^{\max} \quad (39)$$

where $P_{G,n}^{\min}$ and $P_{G,n}^{\max}$ are the upper and lower bounds of technical output of thermal power at bus n.

C. SOLUTION

The formulated bi-level optimization model is a typical mixed-integer nonlinear programming problem (MINP), which can be readily solved by using the branch and bound algorithm. In our study, the commercial solver CPLEX is employed to solve this problem on MATLAB.

In the process of iterative calculation, the upper layer model is firstly calculated to obtain the optimal installed capacity of wind-PV generation and power output of HS, EIL and thermal units, which is passed into the lower layer model as the optimal operating boundary condition. The optimal power output of HS and EIL are calculated to update the result of the upper model. The detailed solution process and procedure of optimal capacity allocation and operation results is shown in Fig. 4.
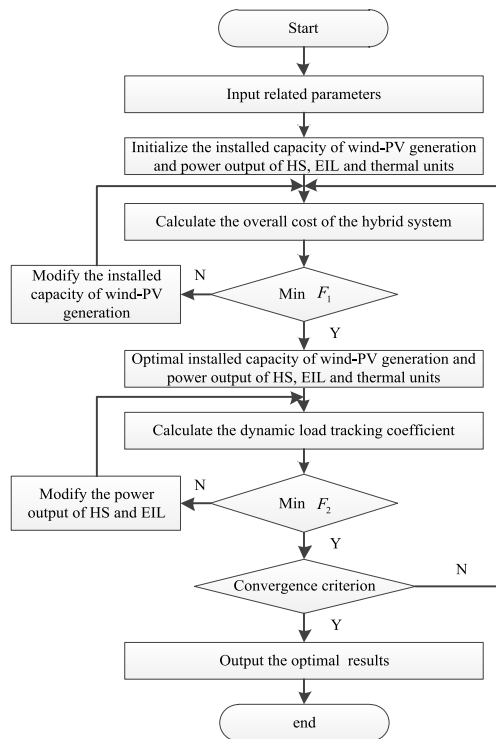
FIGURE 4. The solution procedure of optimal capacity allocation and operation results.

Step 1: Input the system related parameters and initialize the installed capacity of wind-PV generation and power output of HS, EIL and thermal units. Set the iterations $x = 1$ and convergence criterion e;

Step 2: Solve the upper layer model (27) and achieve the objective value A_x, optimal installed capacity of wind-PV generation and power output of HS, EIL and thermal units;

Step 3: Solve the lower layer model (31) and achieve the objective value B_x, optimal power output of HS and EIL. Feedback them to the optimal results of upper model;

Step 4: Normalize A_x and B_x by min-max normalization. If $|(A_x - B_x) - (A_{x+1} - B_{x+1})| \leq e$, the iterative process is converged; if not, continue the iteration, i.e. $x = x + 1$, back to Step 2.

V. SIMULATION RESULTS

A. PARAMETER SETTINGS

To verify the effectiveness of the proposed model, a modified IEEE-14 bus testing system is introduced, where realistic operational data of wind, PV hydro generation and load in Hunan province of China is utilized. Specifically, two thermal generators with capacities of 50 MW and 150 MW are connected to the grid at nodes 1 and 6. The HS in this paper consists of four hydropower stations. The capacities of four hydropower stations at nodes 2, 3, 8 and 9 are 200 MW, 200 MW, 150 MW and 100 MW, respectively. The three controllable EILs are connected to the grid at nodes 4, 5 and 10.

The daily radiation intensity, wind speed and other meteorology data are collected for 5 years data from 1 January 2014 to 31 December 2019 with 1 hour sampling interval, which can be referred to [24]. Through the stochastic modeling method of time series [25], the time series of 8760 hours of load power, unit HS power, unit wind and solar PV generation output are achieved to calculate the optimal capacity of wind and solar PV power. This data processing method based on the definition and identification of the fluctuation process can better keep the variation characteristic of these powers. The optimization results are more suitable for the actual demands of system planning and operation.

The investment cost of wind and solar PV generation are 0.336 million yuan/MW and 0.276 million yuan/MW, respectively. The regulation cost of EIL is 105 yuan/MW. Relevant parameters of EILs are shown in Tables 1.

TABLE 1. Related parameters of EILs.

EIL	Conventional operating power /WM	Maximum operating power /WM	Minimum operating power /WM	Interruption power /WM	Maximum interruption time /h
Load A	45	60	30	8	2
Load B	15	25	10	5	2.5
Load C	10	15	7	2	3

B. OPTIMAL CAPACITY ALLOCATION AND SYSTEM OPERATION RESULTS

By using the proposed bi-level optimization model, the optimal installed capacity of wind and solar PV generation is obtained as 123.5 WM and 154.8 WM, i.e. 14.53% and 18.21% of the total generation capacity of the whole system, respectively. Fig. 5 shows the optimal system operation results under optimal capacity allocation. It can be seen that the peak-valley difference of net load is 233.28 MW and 117.6 MW, which is greater than that of load curve due to the fluctuations of wind and PV power. The net load can be balanced by the regulated power of HS, EIL and thermal units.

At the valley of system load (time 2:00-8:00, 14:00-16:00), the wind power is generated mainly at night and the PV power is generated in the afternoon, of which the maximum power
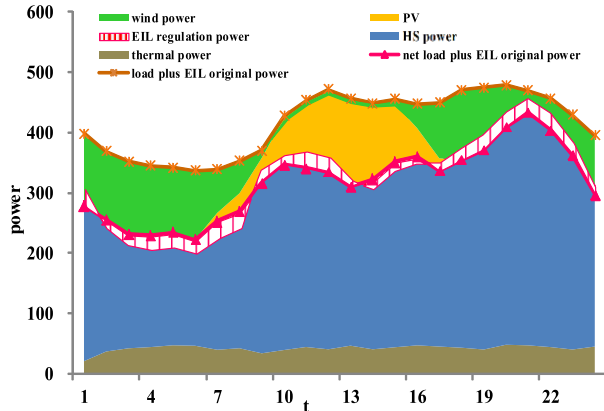
FIGURE 5. Optimal system operation results under optimal capacity allocation.

Cases	Description
1	with HS but without EIL, dynamic regulation and dynamic tracking objective
2	with HS and EIL but without dynamic regulation and dynamic tracking objective
3	with HS, EIL and dynamic regulation but without dynamic tracking objective
4	with HS and EIL, dynamic regulation and dynamic tracking objective

TABLE 3. Optimal results under different cases.

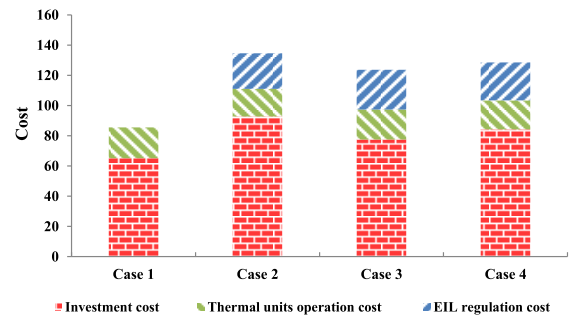| Cases	C_{CON} (million yuan)	C_{DR} (million yuan)	C_G (million yuan)	$\sum_{n=1}^{N} S_{W,n}$ (WM)	$\sum_{n=1}^{N} S_{P,n}$ (WM)	F_2
1	65.10	0	20.5	85.8	131.4	0
2	92.78	23.5	18.3	139.7	166.1	0
3	77.52	26.4	19.8	113.1	143.2	0
4	84.22	25.1	19.2	123.5	154.8	0.69

FIGURE 6. Comparison of overall system cost under four cases.

FIGURE 7. Comparison of permeation levels of wind and solar PV generation under four cases.

is 121.1 MW at time 3:00 and 126.4 MW at time 14:00, respectively. The down-regulation power of HS is reduced to 352.3 MWh during time 2:00-8:00 and 34.2 MWh during time 14:00-16:00. Meanwhile, the up-regulation power of EIL is increased to 148.4 MWh during time 2:00-8:00 and 38.6 MWh during time 14:00-16:00, so as to integrate more renewable energies into the system.

At the peak of system load (time 9:00-13:00, 17:00-1:00), the wind and solar PV generation power is relatively too small to satisfy the load demand, of which the minimum generation is 52.4 MW at time 9:00 and 36.1 MW at time 21:00, respectively. The HS is operated of its full capacity under the current water flow level, of which the up-regulation power is increased to 546.8 MWh during time 9:00-13:00 and 1286.3 MWh during time 17:00-1:00. In the meantime, the down-regulation power of EIL is decreased to 99.2 MWh during time 9:00-13:00 and 212.4 MWh during time 17:00-1:00, so as to complement the deficit power in the system and maintain instant power balance.

As shown in Fig.4, it is obvious that the net load curve in presence of HS and EIL regulation, i.e. the generation curve of thermal units becomes smooth and stable.

C. COMPARATIVE ANALYSIS OF DIFFERENT ALLOCATION MODELS

Case studies are carried out to compare the optimal results obtained by different capacity allocation models. Experimental results are shown in Table 2. The optimal results of wind and solar capacity allocation are reported in Table 3. The penetration level and the overall system cost are shown in Fig. 6 and 7, respectively.

1) IMPACT ANALYSIS ON EIL REGULATION

To illustrate the effects of EIL regulation on improving the penetration of wind and solar PV generation, Cases 1 and 2 are compared. In Case 1, only the HS is regulated to balance the fluctuations of wind and solar PV generation. In Case 2, both HS and EIL are regulated. Moreover, the dynamic regulation ability constraint in (26) and the objective of dynamic

load tracking coefficient expressed in (31) are not considered in the optimization model for both Cases 1 and 2. The regulation of EIL in Case 2 improves the system's ability to smooth the power fluctuations. The obtained optimal installed capacity of wind and solar PV generation in Case 2 is 139.7 MW and 166.1 MW, respectively, which is increased by 53.9 MW and 34.7 MW as compared to Case 1. Detailed results are shown in Fig. 7.

The total cost (including the investment cost and operational cost) in Case 2 is 134.6 million yuan, which is increased

by 49 million yuan, i.e. 36.4%, as comparison to Case 1. The increased part is mainly the investment cost of installed capacity of wind and solar PV generation, accounting for 56.5% of the total increased cost. However, the regulation of EIL has decrease the operational cost of thermal units, which is reduced by 2.2 million yuan, i.e. 4.5%, accordingly.

2) IMPACT ANALYSIS ON DYNAMIC REGULATION CONSTRAINT

As compared to Case 2, Case 3 is used to demonstrate the effects of the dynamic regulation of HS and EIL. The proposed dynamic regulation constraint in (26) is taken into account in the optimization model in Case 3. The total installed capacity of wind and solar PV generation in Case 3 is 256.3 MW, reduced by 49.5 MW, i.e. 16%.

The system dynamic regulation provides better performance in adapting to the power fluctuations, which improves the capacity allocation accuracy of renewable energy to avoid their excessive installation and decreases their curtailed amount. The system regulation ability is illustrated to follow the fluctuation of wind and solar PV generation with or without dynamic regulation, as shown in Table 4. The net load and the system regulation power after the first difference transformation presents the rate of power fluctuation, i.e. ΔP_L^{re} and ΔP_{reg}, respectively. The margin ΔP_{mar} in Table 4 reflects the degree that the regulation rate of system power exceeds the fluctuation rate of the net load, i.e. $\left| \Delta P_{reg} - \Delta P_L^{re} \right|$.

TABLE 4. Comparitive analysis of dynamic system regulation ability.

Time	ΔP_L^{re} (MW/h)	Without dynamic regulation			With dynamic regulation		
		ΔP_{reg} (MW/h)	ΔP_{mar} (MW/h)	P_{WP}^{abon} (MW)	ΔP_{reg} (MW/h)	ΔP_{mar} (MW/h)	P_{WP}^{abon} (MW)
7:00	31.8	31.4	-0.4	3.4	33.4	1.6	0
9:00	48.6	45.5	-3.1	6.3	48.1	-0.5	1.1
10:00	29.7	28.6	-1.1	1.8	33.5	3.8	0
15:00	29.7	29.1	-0.6	2.3	32.5	2.8	0
20:00	38.1	36.5	-1.6	4.7	40.6	2.5	0
22:00	-28.9	-28.3	-0.6	1.6	-30.9	2.0	0
23:00	-41.3	-40.1	-1.2	6.5	-44.1	2.8	0
24:00	-65.6	-61.2	-4.4	19.2	-64.9	-0.7	2.2

It can be seen that the maximum rate of downward fluctuation of net load is 65.6 MW/h at time 24:00 and the maximum rate of upward fluctuation is 48.6 MW/h at time 9:00. If the margin $\Delta P_{mar} > 0$, the system regulation capacity is enough to accommodate the wind and solar PV generation. If $\Delta P_{mar} < 0$, the system regulation cannot follow the fluctuation rate of net load. Thus, wind and solar PV generation should be curtailed. When the dynamic regulation is not adopted, at time 7:00, 9:00, 10:00, 15:00, 20:00, 22:00, 23:00 and 24:00, the total curtailed amount reaches 45.8 MWh. When the dynamic regulation is adopted, the system regulation ability can mostly follow the fluctuation

rate of net load at all the time except 9:00 and 24:00, of which the curtailed amount of wind and solar PV generation become only 3.3 MWh.

3) IMPACT ANALYSIS ON THE DYNAMIC LOAD TRACKING COEFFICIENT

To further illustrate the effects of the dynamic regulation, the proposed objective of dynamic load-tracking coefficient in (31) is considered in the optimization model for Case 4. As compared to Case 3, the total installed capacity and penetration level of wind and solar PV generation are increased by 22 MW and 20MW, respectively, and the total cost is increased by 4.8 million yuan in Case 4. The economic cost difference between Case 3 and 4 is relatively small since the reduced operation and regulation cost offset the increased investment cost.

Based on the above analysis, the optimal wind and solar capacity allocation model for Case 4 is advantageous over other models for Cases 1, 2 and 3. This proposed model aims at the minimum system economic cost and the minimum dynamic load-tracking coefficient with the coordination of dynamic regulation of HS and EIL.

VI. CONCLUSION

This paper proposes a bi-level (planning and operation layers) optimal capacity allocation model for the integrated wind and solar PV generation power in consideration of the dynamic regulation ability of HS and EIL. This model provides a novel method of source-load dynamic coordination to improve the penetration level of renewable energies in the hydro-wind-PV-load systems.

The effectiveness of the proposed model is verified through extensive case studies based on real-world data from a region of Hunan province in China. The results show the proposed method for Case 4 provides better performance in adapting to the power fluctuations, which improves the capacity allocation of renewable energy and decreases their curtailed amount as compared to other methods for Cases 1, 2 and 3. The installed capacity of wind and solar PV generation reaches 123.5 WM and 154.8 WM, i.e. 14.53% and 18.21% of the total generation capacity of the whole system, respectively.

In addition, integrating wind and PV power with cascade hydropower will be more complex. How to divide the total output of hydropower cascades into the single hydropower station will be considered in our future work.

REFERENCES

[1] National Energy Administration, China. (Jan. 2019). *The Integrated Operation Introduction of Renewable Energies in 2018.* [Online]. Available: http://www.nea.gov.cn/2019-01/28/c_137780519.html

[2] M. J. Sanjari, H. B. Gooi, and N.-K.-C. Nair, "Power generation forecast of hybrid PV–wind system," *IEEE Trans. Sustain. Energy*, vol. 11, no. 2, pp. 703–712, Apr. 2020, doi: 10.1109/TSTE.2019.2903900.

[3] T. G. Hlalele, R. M. Naidoo, J. Zhang, and R. C. Bansal, "Dynamic economic dispatch with maximal renewable penetration under renewable obligation," *IEEE Access*, vol. 8, pp. 38794–38808, Feb. 2020.

[4] J. Ekstrom, M. Koivisto, I. Mellin, R. J. Millar, and M. Lehtonen, "A statistical model for hourly large-scale wind and photovoltaic generation in new locations," *IEEE Trans. Sustain. Energy*, vol. 8, no. 4, pp. 1383–1393, Oct. 2017.

[5] D. Bian, D. Shi, M. Pipattanasomporn, M. Kuzlu, and S. Rahman, "Mitigating the impact of renewable variability with demand-side resources considering communication and cyber security limitations," *IEEE Access*, vol. 7, pp. 1379–1389, Dec. 2019.

[6] P. P. Biswas, P. N. Suganthan, B. Y. Qu, and G. A. J. Amaratunga, "Multiobjective economic-environmental power dispatch with stochastic wind-solar-small hydro power," *Energy*, vol. 150, pp. 1039–1057, May 2018.

[7] J. Jurasz, J. Mikulik, M. Krzywda, B. Ciapała, and M. Janowski, "Integrating a wind- and solar-powered hybrid to the power system by coupling it with a hydroelectric power station with pumping installation," *Energy*, vol. 144, pp. 549–563, Feb. 2018.

[8] A. J. H. van Meerwijk, R. M. J. Benders, A. Davila-Martinez, and G. A. H. Laugs, "Swiss pumped hydro storage potential for Germany's electricity system under high penetration of intermittent renewable energy," *J. Mod. Power Syst. Clean Energy*, vol. 4, no. 4, pp. 542–553, Oct. 2016.

[9] B. Ming, P. Liu, S. Guo, X. Zhang, M. Feng, and X. Wang, "Optimizing utility-scale photovoltaic power generation for integration into a hydropower reservoir by incorporating long- and short-term operational decisions," *Appl. Energy*, vol. 204, pp. 432–445, Oct. 2017.

[10] X. B. Wang, J. Chang, X. Meng, and Y. Wang, "Hydro-thermal-wind-photovoltaic coordinated operation considering the comprehensive utilization of reservoirs," *Energy Convers. Manage.*, vol. 198, no. 10, p. 11824, Oct. 2019.

[11] Y. Zhang, C. Ma, J. Lian, X. Pang, Y. Qiao, and E. Chaima, "Optimal photovoltaic capacity of large-scale hydro-photovoltaic complementary systems considering electricity delivery demand and reservoir characteristics," *Energy Convers. Manage.*, vol. 195, pp. 597–608, Sep. 2019.

[12] S. R. Konda, L. K. Panwar, B. K. Panigrahi, and R. Kumar, "Optimal offering of demand response aggregation company in price-based energy and reserve market participation," *IEEE Trans. Ind. Informat.*, vol. 14, no. 2, pp. 578–587, Feb. 2018.

[13] N. Javaid, G. Hafeez, S. Iqbal, N. Alrajeh, M. S. Alabed, and M. Guizani, "Energy efficient integration of renewable energy sources in the smart grid for demand side management," *IEEE Access*, vol. 6, pp. 77077–77096, Aug. 2018.

[14] X. Li, X. Cao, C. Li, B. Yang, M. Cong, and D. Chen, "A coordinated peak shaving strategy using neural network for discretely adjustable energy-intensive load and battery energy storage," *IEEE Access*, vol. 8, pp. 5331–5338, Dec. 2020.

[15] J. Zhang, P. Zhang, H. Wu, X. Qi, S. Yang, and Z. Li, "Two-stage load-scheduling model for the incentive-based demand response of industrial users considering load aggregators," *IET Gener., Transmiss. Distrib.*, vol. 12, no. 14, pp. 3518–3526, Aug. 2018.

[16] Y. Bao, J. Xu, S. Liao, Y. Sun, X. Li, Y. Jiang, D. Ke, J. Yang, and X. Peng, "Field verification of frequency control by energy-intensive loads for isolated power systems with high penetration of wind power," *IEEE Trans. Power Syst.*, vol. 33, no. 6, pp. 6098–6108, Nov. 2018.

[17] S. Liao, J. Xu, Y. Sun, Y. Bao, and B. Tang, "Control of energy-intensive load for power smoothing in wind power plants," *IEEE Trans. Power Syst.*, vol. 33, no. 6, pp. 6142–6154, Nov. 2018.

[18] K. Bruninx, Y. Dvorkin, E. Delarue, W. D'haeseleer, and D. S. Kirschen, "Valuing demand response controllability via chance constrained programming," *IEEE Trans. Sustain. Energy*, vol. 9, no. 1, pp. 178–187, Jan. 2018.

[19] M. Barani, M. Shafie-khah, A. A. S. de la Nieta, and J. P. S. Catalão, "Risk-constrained offering strategy for aggregated hybrid power plant including wind power producer and demand response provider," *IEEE Trans. Sustain. Energy*, vol. 7, no. 2, pp. 513–525, Apr. 2016.

[20] H. Jin, Z. Li, H. Sun, Q. Guo, R. Chen, and B. Wang, "A robust aggregate model and the two-stage solution method to incorporate energy intensive enterprises in power system unit commitment," *Appl. Energy*, vol. 206, pp. 1364–1378, Nov. 2017.

[21] J. Xu, Y. Chen, S. Liao, Y. Sun, L. Yao, H. Fu, X. Jiang, D. Ke, X. Li, J. Yang, and X. Peng, "Demand side industrial load control for local utilization of wind power in isolated grids," *Appl. Energy*, vol. 243, pp. 47–56, Jun. 2019.

[22] H. Jiang, J. Lin, Y. Song, W. Gao, Y. Xu, B. Shu, X. Li, and J. Dong, "Demand side frequency control scheme in an isolated wind power system for industrial aluminum smelting production," *IEEE Trans. Power Syst.*, vol. 29, no. 2, pp. 844–854, Mar. 2014.

[23] H. Yang, J. Zhang, J. Qiu, S. Zhang, M. Lai, and Z. Y. Dong, "A practical pricing approach to smart grid demand response based on load classification," *IEEE Trans. Smart Grid*, vol. 9, no. 1, pp. 179–190, Jan. 2018.

[24] *National Meteorological Science Data Center*. Accessed: Dec. 2019. [Online]. Available: http://data.cma.cn/

[25] C. Liu, C. Li, Y. Huang, and Y. Wang, "A novel stochastic modeling method of wind power time series considering the fluctuation process characteristics," *J. Renew. Sustain. Energy*, vol. 8, no. 3, May 2016, Art. no. 033304.

HONGMING YANG (Member, IEEE) received the M.S. degree in electrical engineering from Wuhan University, in 1997, and the Ph.D. degree in electrical engineering from the Huazhong University of Science and Technology, in 2003. She was a Research Associate with the Hong Kong Polytechnic University, in 2009 and 2010, and also a Research Fellow with the University of Newcastle, in 2013 and 2014. She is currently a Full Professor with the Changsha University of Science and Technology. Her research interests include power system analysis and power markets.

QIAN YU is currently pursuing the Ph.D. degree with the School of Economics and Management, Changsha University of Science and Technology, Changsha, China. Her current research interests include renewable energy permeation and power system optimization.

JUNPENG LIU is currently pursuing the M.S. degree in electrical engineering with the Changsha University of Science and Technology, Changsha, China. His current research interests include renewable energy permeation and power system optimization.

YOUWEI JIA (Member, IEEE) received the B.Eng. degree from Sichuan University, China, in 2011, and the Ph.D. degree from The Hong Kong Polytechnic University, Hong Kong, in 2015. From 2015 to 2018, he was a Postdoctoral Fellow of The Hong Kong Polytechnic University. He is currently an Assistant Professor with the Department of Electrical and Electronics Engineering, Southern University of Science and Technology, Shenzhen, China. His research interests include microgrid, renewable energy modeling and control, power system security analysis, complex networks, and artificial intelligence in power engineering.
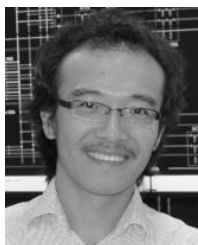
GUANGYA YANG (Senior Member, IEEE) received the B.E., M.E., and Ph.D. degrees in electric power system in 2002, 2005, and 2008, respectively. He is currently an Associate Professor with the Center for Electric Power and Energy, Department of Electrical Engineering, Technical University of Denmark, Kongens Lyngby, Denmark. Since 2009, he has been with the Technical University of Denmark as a Post-doctoral Researcher and has been leading several industrial collaborative projects in Denmark in the fields of monitoring, operation, and the protection of renewable energy systems. His research interests include renewable energy integration, smart grids, and cyber-physical energy systems.

ZHAO YANG DONG (Fellow, IEEE) received the Ph.D. degree from the University of Sydney, Australia, in 1999. He is currently a SHARP Professor with the University of New South Wales (NSW), Australia. His immediate role is a Professor and the Head of the School of Electrical and Information Engineering, University of Sydney. He was previously the Ausgrid Chair and the Director of the Ausgrid Centre for Intelligent Electricity Networks (CIEN), The University of Newcastle, Australia. He also held academic and industrial positions at The Hong Kong Polytechnic University and Transend Networks (now TAS-Networks), Tas, Australia. His research interests include smart grid, power system planning, power system security, load modeling, renewable energy systems, electricity market, and computational intelligence and its applications in power engineering. He is an Editor of the IEEE TRANSACTIONS ON SMART GRID, the IEEE POWER ENGINEERING LETTERS, and *IET Renewable Power Generation*.

• • •

EMMANUEL ACKOM received the Ph.D. degree from the Brandenburg University of Technology (BTU), Germany, in 2005, through the Interdisciplinary Environment and Resource Management Programme. He is currently a Senior Energy and Climate Expert with the UNEP DTU Partnership, Technical University of Denmark. His research interests include intersection of clean energy policy and technologies, socio-economic development, and environmental sustainability with a particular emphasis on developing countries.